

Skyrme–Hartree–Fock approach to the change of level occupancy of low mass halo nuclei

RUPAYAN BHATTACHARYA

Gurudas College, Narikeldanga, Calcutta 700 054, India

MS received 29 January 1999

Abstract. With a new parameterization of potential parameters which reproduces the ground state properties of shell closed nuclei fairly accurately, the role of occupancy of $2s_{1/2}$ level in determining the halo structures of ^{17}O , ^{16}N , ^{15}C , ^{14}B , ^{13}Be have been investigated. The results show interesting cross over of level occupancies which may explain the increase in interaction radii.

Keywords. Skyrme interaction; occupancy; one-neutron halo.

PACS Nos 21.60.Jz; 21.10.Dr; 21.10.Pc

1. Introduction

Availability of radioactive nuclear beams has opened up new areas of intense research. It has been found recently that single particle level inversion between $1d_{5/2}$ and $2s_{1/2}$ in $N = 9$ isotones is the cause of development of a neutron halo in the mass range of $A = 13$ to $A = 17$. However, there are not many theoretical attempts to shed light on this problem. Using shell model calculation, Fortune [1] tried to evaluate the level positions of ^{15}C , ^{16}N and ^{17}O . But no attempt was made to correlate the level structure with the formation of neutron halo. Through the relativistic mean field approach, Ren *et al* [2] could reproduce the binding energies, rms radii to a good extent, yet it did not show the change of occupation probabilities of the last neutron in the $N = 9$ isotones.

In this paper, we show through another kind of well tested mean field calculation how level inversion of $1d_{5/2}$ and $2s_{1/2}$ happens as we move from $N = 9$ isotones ^{17}O to ^{13}B . The information gathered so far from experiments [3–5] show that $N = 8$ isotones from ^{16}O to ^{12}Be are spherical nuclei because of the magicity of $N = 8$. Deformation produced by the addition of an extra loosely bound neutron will not be significant as has been verified by theoretical calculations [1,6]. Also deformed RMF calculations [2] have confirmed that deformations are not important for these nuclei. Hence, we have performed spherical Skyrme–Hartree–Fock with BCS approach type calculations for this region.

2. Method

The potential used has the following form [7]

$$\begin{aligned}
 V(\mathbf{r}_1 - \mathbf{r}_2) = & t_0(1 + x_0 P_\sigma) \delta(\mathbf{r}_1 - \mathbf{r}_2) + \frac{1}{2} t_1(1 + x_1 P_\sigma)(k^2 - k'^2) \delta(\mathbf{r}_1 - \mathbf{r}_2) \\
 & + t_2(1 + x_2 P_\sigma) k' \delta(\mathbf{r}_1 - \mathbf{r}_2) k + 1/6 t_3 \rho^\alpha (1 + x_3 P_\sigma) \delta(\mathbf{r}_1 - \mathbf{r}_2) \\
 & + i t_4 k' \delta(\mathbf{r}_1 - \mathbf{r}_2) (\mathbf{r} \times \mathbf{k}).
 \end{aligned} \tag{1}$$

The Hartree–Fock equation resulting from the force is

$$h_q R_\beta = \epsilon_\beta R_\beta \tag{2}$$

with

$$h_q = \partial_r B_q \partial_r + U_q + U_{1s,q} l \cdot s, \tag{3}$$

where

$$\begin{aligned}
 B_q = & h^2/2m_q + 1/8[t_1(1 + (1/2)x_1) + t_2(1 + (1/2)x_2)]\rho \\
 & - 1/8[t_1(1/2 + x_1) - t_2(1 + x_2)]\rho_q,
 \end{aligned} \tag{4}$$

and

$$\begin{aligned}
 U_q = & t_0(1 + (1/2)x_0)]\rho - t_0(1/2 + x_0)]\rho_q + 1/12 t_3 \rho^\alpha [(2 + a)(1 + (1/2)x_3)\rho \\
 & - 2(1/2 + x_3)\rho_q - \alpha(1/2 + x_3)(\rho_p^2 + \rho_n^2)/\rho] + 1/4[t_1(1 + (1/2)x_1) \\
 & + t_2(1 + (1/2)x_2)]\tau - 1/4[t_1(1/2 + x_1) - t_2(1/2 + x_2)]\tau_q \\
 & - 1/8[3t_1(1 + (1/2)x_1) - t_2(1 + (1/2)x_2)]\Delta\rho + 1/8[3t_1(1/2 + x_1) \\
 & + t_2(1/2 + x_2)]\Delta\rho_q - 1/2 t_4 (\nabla J + \nabla J_q) + U_{\text{coul}},
 \end{aligned} \tag{5}$$

$$U_{1s,q} = (1/4)t_4(\rho + \rho_q) + 1/8(t_1 - t_2)J_q - 1/8(x_1 t_1 + x_2 t_2)J. \tag{6}$$

The Coulomb energy is given by

$$E_{\text{coul}} = (1/2)e^2 d^3 r d^3 r' \rho_c(r) [1/|r - r'|] \rho_c(r') + E_{\text{coul,exch}}. \tag{7}$$

In the spherical representation

$$\rho_q(r) = \sum_{nlj} w_\beta (2j_\beta + 1) / 4\pi [R_\beta / r]^2, \tag{8}$$

$$\tau_q(r) = \sum_{nlj} w_\beta (2j_\beta + 1) / 4\pi [(\partial_r R_\beta / r)^2 + l(l + 1) / r^2 (R_\beta / r)^2], \tag{9}$$

$$\nabla J_q(r) = [\partial_r + 2/r] J_q(r), \tag{10}$$

Table 1a. Parameter set of the potential.

t_0	t_1	t_2	t_3	t_4
-2930.0	325.11	-339.41	18700.09	100.0

Table 1b.

x_0	x_1	x_2	x_3	α
0.25921	0.64981	-0.53732	0.18079	0.1666667

$$J_q(r) = \sum_{nlj} w_\beta (2j_\beta + 1) / 4\pi [j_\beta(j_\beta + 1) - l_\beta(l_\beta + 1) - 3/4] 2/r [R_\beta/r]^2. \quad (11)$$

The parameters of the potential (SKPNEW) are shown in table 1.

3. Results

We have evaluated the total binding energies of the nuclei, RMS matter, charge and neutron radii, single particle energies near the Fermi surface, separation energies of the last neutron and the occupation probabilities of the last neutron. We have not made any ad hoc adjustments of placing the last neutron in any specific level. The results of these calculations are shown in tables 2 and 3. One can observe that the agreement of the calculated binding energies and experimental binding energies for ^{17}O and ^{15}C is excellent. However, in the cases of ^{16}N , ^{14}Be and ^{13}B , theoretical binding energies are slightly more than the experimental values.

It is apparent from the tables that the calculated RMS radii for the $N = 9$ isotone nuclei show the correct trend, though in some cases comparison could not be made due to lack of experimental results. One important observation is that the level spacing between $1d_{5/2}$ and $2s_{1/2}$ states decreases monotonously with the increase of $N - Z$. Another interesting feature is the formation of one neutron halo by the pushed out neutron in the $2s_{1/2}$ state. It is known from the experiments that the last neutron of ^{17}O is in the $1d_{5/2}$ state and that in ^{15}C is in $2s_{1/2}$ state. The spin and parity of the ground state of ^{16}N is 2^- and this confirms that the last neutron in ^{16}N occupies the $1d_{5/2}$ level. Calculated occupation probabilities support this fact. According to our calculation the last neutron in ^{14}B should occupy $2s_{1/2}$ level. This is in good correspondence with the relativistic mean field calculation of Ren *et al.* Another important point to note is the appearance of one-neutron halo along with the level inversion between $1d_{5/2}$ and $2s_{1/2}$ for the ground states of ^{15}C and ^{14}B . A possible cause of this level inversion in these neutron rich nuclei is the influence of isospin degree of freedom. The large value of $N - Z$ may influence the level spacings which in turn pushes the wave function out. In that case total binding energy will play an important role.

Table 2. Skyrme–Hartree–Fock results for $N = 9$ isotones.

	^{17}O	^{16}N	^{15}C	^{14}B	^{13}Be
B.E. (MeV)	131.01	120.65	106.20	90.12	71.04
B.E. _{ex} (MeV)	131.76	117.98	106.50	85.42	66.64
R (fm)	2.77	2.76	2.77	2.83	2.97
R_{ex} (fm)		2.71 ± 0.28	2.78 ± 0.09	3.00 ± 0.10	
R_p (fm)	2.72	2.65	2.56	2.48	2.39
R_p^{ex} (fm)	2.72 ± 0.02	2.61 ± 0.01	2.56 ± 0.05		
R_n (fm)	2.81	2.84	2.89	3.00	3.20
R_n^{ex} (fm)		2.79 ± 0.50	2.94 ± 0.15	3.27 ± 0.16	

Experimental values are taken from Ren *et al* [2].

Table 3. Single particle (n) energies and occupation probabilities of the neutron states.

	^{17}O	^{16}N	^{15}C	^{14}B	^{13}Be
$\epsilon_{2s_{1/2}}$	-4.43	-2.95	-1.54	-0.27	0.79
$S_{2s_{1/2}}$	0.16	0.10	0.16	0.17	0.21
$\epsilon_{1d_{5/2}}$	-5.83	-3.94	-2.00	-0.02	1.88
$S_{1d_{5/2}}$	0.21	0.16	0.13	0.15	0.14

Table 4. A comparative study of the single particle energy difference $\Delta (= \epsilon_{1d_{5/2}} - \epsilon_{2s_{1/2}}$ of two states near the Fermi surface.

	^{17}O	^{16}N	^{15}C	^{14}B	^{13}Be
$-\Delta$ (MeV)	1.4	0.99	0.46	-0.25	-1.09
$-\Delta_{\text{ex}}$ (MeV)		0.87	0.15	-0.74	

Table 5. The variation of neutron separation energies and neutron skin thickness with neutron excess.

$N - Z$	$S_n(\text{ex})$ (MeV)	S_n (MeV)	$R_n - R_p$ (fm)
1	4.14	8.58	0.09
2	2.49	6.55	0.19
3	1.22	3.91	0.31
4	0.97	2.66	0.52
5		0.76	0.81

In order to bring out the details of the structure of the nuclei under study, we have plotted the density distributions of matter, proton and neutron for the ground state of ^{17}O , ^{16}N , ^{15}C and ^{14}B (figure 1). One can see the formation of one-neutron halo in ^{15}C and ^{14}B . In order to emphasize the importance of spin-orbit force, we have made a comparative study of the difference $\Delta = \epsilon(1d_{5/2}) - \epsilon(2s_{1/2})$ for all the nuclei studied (table 4). Lastly, in table 5 we have presented the variation of neutron separation energies and neutron skin thickness with neutron excess for the ground state of $N = 9$ isotones. The appearance of neutron halos in ^{15}C and ^{14}B is quite apparent, however, the calculation is not able to reproduce the neutron separation energies.

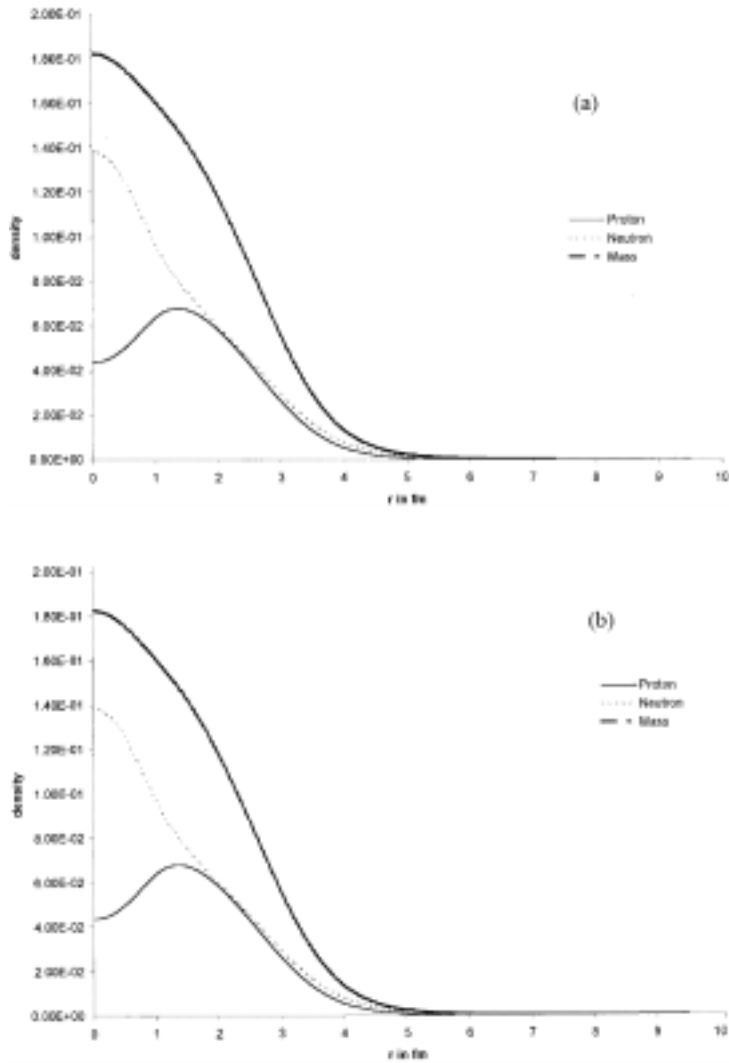


Figure 1a, b.

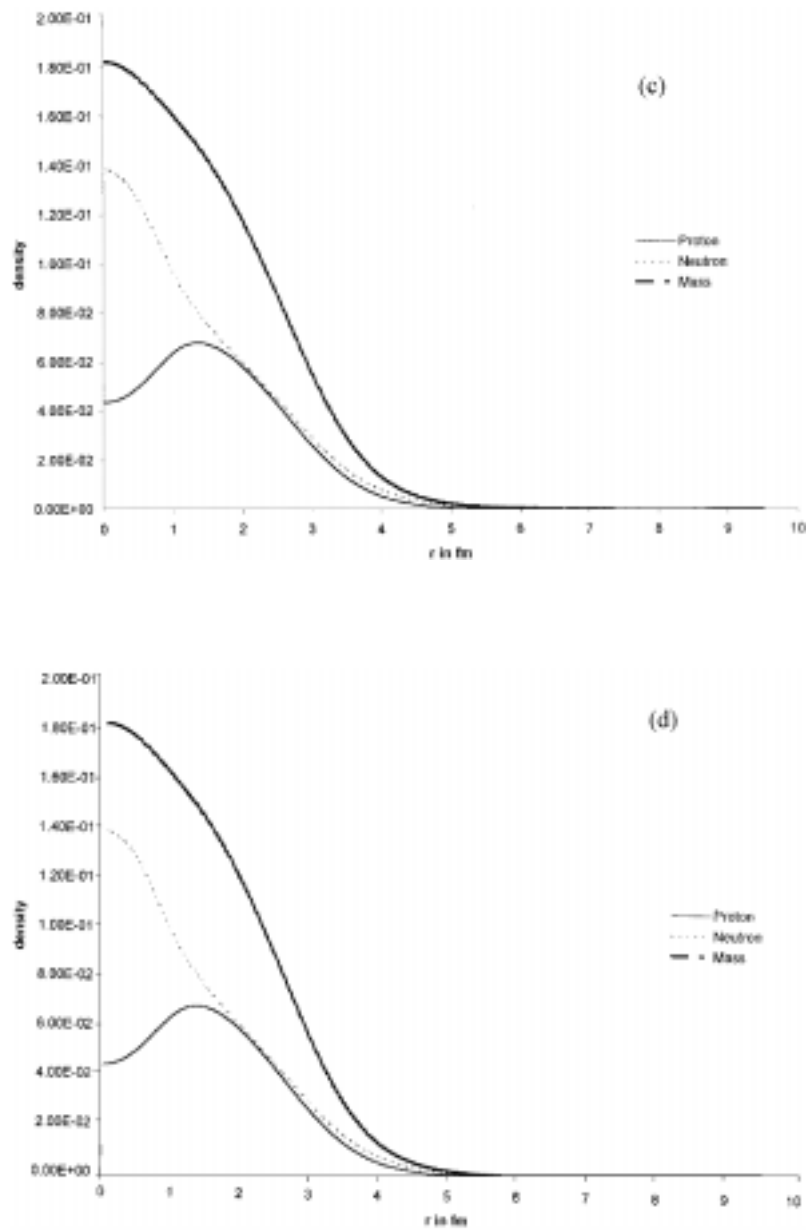


Figure 1c, d.

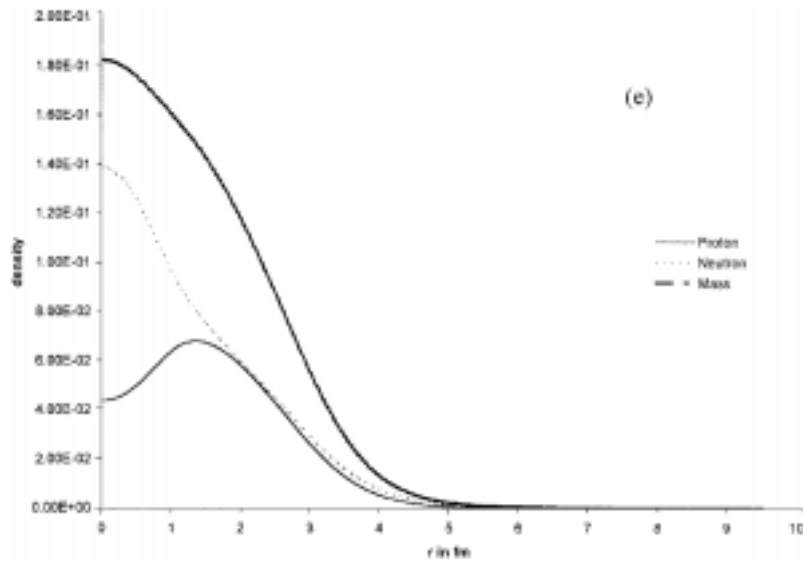


Figure 1a–e. Proton, neutron and mass distribution of (a) ^{13}Be , (b) ^{14}B , (c) ^{15}C , (d) ^{16}N and (e) ^{17}O .

4. Conclusion

Through Skyrme type interaction we have calculated the ground state properties of $N = 9$ isotones. Reasonably good agreement has been obtained with the experimental results for these nuclei near the drip line. Isospin degree of freedom is expected to cause the level inversion and formation of one-neutron halo in this region. The study is being extended to other regions of interest.

References

- [1] H T Fortune, *Phys. Rev.* **C52**, 2261 (1995)
- [2] Z Ren, B Chen, Z Ma and G Xu, *Z. Phys.* **A357**, 137 (1997)
- [3] F Ajzenberg-Selove, *Nucl. Phys.* **A523**, 1 (1991)
- [4] F Ajzenberg-Selove, *Nucl. Phys.* **A460**, 1 (1986)
- [5] D R Tilley, H R Weller and C M Cheves, *Nucl. Phys.* **A564**, 1 (1993)
- [6] I Talmi and I Unna, *Phys. Rev. Lett.* **4**, 469 (1960)
- [7] J Bartel, P Quentin, M Brack, C Guet and H B Hakansson, *Nucl. Phys.* **A386**, 79 (1982)